J|A|C|S
ARTICLES
Published on Web 05/10/2002

Assembly of α-helical Peptide Coatings on Hydrophobic Surfaces

Joanna R. Long,[†] Nathan Oyler,[‡,§] Gary P. Drobny,[*,‡] and Patrick S. Stayton[†]

Contribution from the Department of Bioengineering and the Department of Chemistry, University of Washington, Seattle, Washington 98195

Received July 3, 2001. Revised Manuscript Received January 23, 2002

Abstract: The adsorption or covalent attachment of biological macromolecules onto polymer materials to improve their biocompatibility has been pursued using a variety of approaches, but key to understanding their efficacy is the verification of the structure and dynamics of the immobilized biomolecules. Here we present data on peptides designed to adsorb from aqueous solutions onto highly porous hydrophobic surfaces with specific helical secondary structures. Small linear peptides composed of alternating leucine and lysine residues were synthesized, and their adsorption onto porous polystyrene surfaces was studied using a combination of solid-state NMR techniques. Using conventional solid-state NMR experiments and newly developed double-quantum techniques, their helical structure was verified. Large-amplitude dynamics on the NMR time scale were not observed, suggesting irreversible adsorption of the peptides. Their association, adsorption, and structure were examined as a function of helix length and sequence periodicity, and it was found that, at higher solution concentrations, peptides as short as seven amino acids adsorb with defined secondary structures. Two-dimensional double-quantum experiments using ^{13}C-enriched peptide sequences allow high-resolution determination of secondary structure in heterogeneous environments where the peptides are a minor component of the material. These results shed light on how polymeric surfaces may be surface-modified by structured peptides and demonstrate the level of molecular structural and dynamic information solid-state NMR can provide.

Introduction

The development of materials with enhanced biocompatibility is a major focus of the materials and tissue engineering communities.[1−4] There has thus been considerable interest in the use of peptide- and protein-based coatings on materials and tissue engineering scaffolds, with the goal of recreating a natural extracellular matrix (ECM) to direct wound repair or tissue development and homeostasis.[5−9] Many of the current materials used in biomedical materials and tissue-engineering scaffolds are hydrophobic in nature. These surfaces can be modified directly with biomolecules, or the biomolecules can be conjugated through a hydrophilic layer (e.g., PEO-based).[10−15] In addition to the biomaterials and tissue engineering fields, there is considerable interest in the immobilization of active peptides and proteins, often again on relatively hydrophobic material platforms, in affinity separations, diagnostics, proteomics, and cell culture technologies. A major concern in all these applications is retention of biological specificity (i.e., structure, or dynamics, or both) upon adsorption. This aim is at odds with what is generally observed when proteins passively adsorb onto hydrophobic surfaces; adsorption often leads to loss of biological functionality.

We report here an approach to modifying hydrophobic materials using synthetic peptides that are designed to assemble with a defined structure and orientation on the surface via the hydrophobic effect. These peptides reverse the usual paradigm of protein unfolding being driven by hydrophobic surfaces, through the design of a recognition mechanism that stabilizes a

* To whom correspondence should be addressed. (G.P.D.) Phone: (206) 685-2052. Fax: (206) 685-2052. E-mail: drobny@chem.washington, edu. Also, (J.R.L.) Phone: (206) 685-2052. Fax: (206) 685-2052. E-mail: jrlong@u.washington.edu. (P.S.S. Phone: (206) 685-8148. Fax: (206) 685-8256. E-mail: stayton@u.washington.edu.

† Department of Bioengineering, University of Washington.

‡ Department of Chemistry, University of Washington.

§ Present address: Laboratory of Chemical Physics, National Institute of Diabetes and Digestive and Kidney Diseases, National Institutes of Health, Bethesda, MD 20892.

(1) Healy, K. E. *Curr. Opin. Solid State Mater. Sci.* **1999**, *4*, 381−387.
(2) Angelova, N.; Hunkeler, D. *Trends Biotechnol.* **1999**, *17*, 409−421.
(3) Griffith, L. G. *Acta Mater.* **2000**, *48*, 263−277.
(4) Langer, R. *Acc. Chem. Res.* **2000**, *33*, 94−101.
(5) 5. Borkenhagen, M.; Clemence, J. F.; Sigrist, H.; Aebischer, P. J. *Biomed. Mater. Res.* **1998**, *40*, 392−400.
(6) Belcheva, N.; Baldwin, S. P.; Saltzman, W. M. *J. Biomater. Sci., Polym. Ed.* **1998**, *9*, 207−226.
(7) Rezania, A.; Healy, K. E. *Biotechnol. Prog.* **1999**, *15*, 19−32.
(8) Gilbert, M.; Shaw, W. J.; Long, J. R.; Nelson, K.; Drobny, G. P.; Giachelli, C. M.; Stayton, P. S. *J. Biol. Chem.* **2000**, *275*, 16213−16218.
(9) Whang, K.; Goldstick, T. K.; Healy, K. E. *Biomaterials* **2000**, *21*, 2545−2551.
(10) Drumheller, P. D.; Elbert, D. L.; Hubbell, J. A. *Biotechnol. Bioeng.* **1994**, *43*, 772−780.
(11) Walluscheck, K. P.; Steinhoff, G.; Kelm, S.; Haverich, A. *Eur. J. Vasc. Endovasc. Surg.* **1996**, *12*, 321−330.
(12) Neff, J. A.; Caldwell, K. D.; Tresco, P. A. *J. Biomed. Mater. Res.* **1998**, *40*, 511−519.
(13) Tong, Y. W.; Shoichet, M. S. *J. Biomater. Sci., Polym. Ed.* **1998**, *9*, 713−729.
(14) Pakalns, T.; Haverstick, K. L.; Fields, G. B.; McCarthy, J. B.; Mooradian, D. L.; Tirrell, M. *Biomaterials* **1999**, *20*, 2265−2279.
(15) Bhadriraju, K.; Hansen, L. K. *Biomaterials* **2000**, *21*, 267−272.

specific secondary structure on the surface. Degrado and Lear[16] demonstrated that specific secondary structures could be observed in short peptides at the air/water interface by varying the hydrophobic periodicity in the peptides to match the periodicity of the desired secondary structure. If these peptides were to fold into the defined secondary structures on hydrophobic surfaces, they might then be used as surface adaptors on which to display other short peptide sequences or protein fragments. The defined orientation of the peptides could promote the display of sequences that instruct cells through specific cell receptors, or peptide/protein domains, to be used in diagnostics or proteomics technology.

It was shown previously in solution and at the air/water interface that the periodicity of hydrophobic and hydrophilic residues can be more important than the helical propensity of a particular amino acid in determining peptide secondary structure, especially at concentrations high enough for aggregation to occur.[17−23] This principle should be magnified when peptides adsorb on hydrophobic surfaces where the planar environment restricts the conformational degrees of freedom.[24,25] To test this hypothesis, we synthesized peptides with varying periodicities of leucine and lysine residues, corresponding to the underlying periodicities of α- and 3_{10}-helices. We also investigated the dependence of helical structure stability on peptide length by designing short helices of 7−8 amino acids in length and longer helices consisting of 13−14 amino acids. The peptide sequences and isotope enrichment at the backbone carbonyl carbons for NMR observation (indicated in boldface type) are as follows:

$LK3_{10}7$: Ac-LLK**LL**KL-NH_2

Lkα8: Ac-LLKK**LL**KL-NH_2

$LK3_{10}13$: Ac-LLK**LL**KLLKLLKL-NH_2

Lkα14: Ac-LKKLLK**LL**KKLLKL-NH_2

Solid-state NMR (SSNMR) has the ability to probe structure and dynamics at specific residues in a peptide sequence. These experiments can be carried out on systems under controlled conditions, allowing the investigation of temperature, pH, solvent, and buffering effects on peptide structure. Understanding peptide structure and dynamics on surfaces at a fundamental, molecular level will provide insight into optimizing their functional properties. We have applied a suite of cross-polarization magic angle spinning (CPMAS) and dipolar recoupling SSNMR techniques that directly determine the backbone torsion angles ((φ, ψ) of the surface-immobilized and hydrated peptides.

Materials and Methods

Peptide Synthesis and Characterization. Carbonyl ^{13}C-labeled leucine was purchased from Cambridge Isotope Laboratories (Andover, MA) and protected using standard protocols. Peptides were synthesized by United Biochemical Research, Inc. (Seattle, WA) on an automated synthesizer using MBHA resin and protected, isotopically labeled amino acids provided by the authors. The peptides were cleaved from the resin using 95% trifluoroacetic acid with 2.5% triisopropylsilane and 2.5% water. The crude peptides were purified using a Waters HPLC C-18 reversed-phase column with a water/acetonitrile solvent system containing 0.1% trifluoroacetic acid. Peptide fractions were lyophilized and analyzed by electrospray mass spectrometry to establish isotope incorporation and peptide purity.

Peptide Adsorption to Polystyrene and NMR Sample Preparation. Peptides were adsorbed to polystyrene by adding 10−20 mL of a solution of 1−5 mM peptide in water to 250 mg of polystyrene resin with a surface area of 700 m^2/g (Tosohaas, Stuttgart, Germany). The mixture was shaken for 24−48 h followed by the removal of the peptide-coated resin via centrifugation. The resin was subsequently washed repeatedly with water. Unadsorbed peptide samples were prepared by lyophilizing peptides from solutions of 100 μM to 10 mM concentration.

SSNMR Studies. Chemical shift spectra were taken using CPMAS on a home-built spectrometer operating at a ^{13}C frequency of 125.74 MHz using a home-built, triply resonant MAS probe. These experiments employed a ^1H 90° pulse width of 4 μs followed by a contact time of 2 ms. Spectra were acquired at spinning speeds of 3000 and 4000 Hz. A total of 128 scans were acquired for the samples off the surface. The samples on the surface were signal-averaged for 512 scans. The chemical shifts were referenced externally to the crystalline tripeptide AGG using values previously reported.[26] Fitting the spectra acquired at 3000 and 4000 Hz and then averaging the results determined the principal values of the chemical shift tensors.

Dipolar recoupling with a windowless sequence (DRAWS)[27,28] experiments were carried out on a home-built spectrometer operating at a ^{13}C NMR frequency of 100.7 MHz using a home-built quadruply resonant MAS probe. Cross-polarization was generated with a 4-μs ^1H 90° pulse followed by a 2-ms mixing time. The DRAWS pulse sequence consists of a windowless pulse train applied in synchrony with the rotor cycle. The transverse magnetization is then observed stroboscopically every four rotor cycles and normalized with respect to the magnetization observed without any DRAWS dephasing. A ^{13}C rf field of 34.0 kHz, corresponding to a 7.35-μs π/2 pulse, was used during the DRAWS mixing period, with proton decoupling of >110 kHz applied throughout the DRAWS and acquisition periods. The samples were spun at 4000 ± 5 Hz to match with the 250-μs DRAWS cycle time. Each DRAWS experiment was run at least 5 times, using either 128 or 512 scans per spectrum and a repetition time of 4 s. Adsorbed samples consisted of ∼10 mg of peptide adsorbed to 100 mg of polystyrene packed into a 5-mm rotor. Simulated DRAWS decay curves were calculated using numerical methods that incorporated the observed relaxation times from singly labeled peptides, chemical shift anisotropies, and experimental parameters.

DQDRAWS[29,30] experiments were carried out on home-built spectrometers operating at a ^{13}C NMR frequencies of 125.72 and 100.6 MHz. Cross-polarization was generated with a 4-μs ^1H 90 followed by

(16) Degrado, W. F.; Lear, J. D. *J. Am. Chem. Soc.* **1985**, *107*, 7684−7689.
(17) Xiong, H.; Buckwalter, B. L.; Shieh, H. M.; Hecht, M. H. *Proc. Natl. Acad. Sci. U.S.A.* **1995**, *92*, 6349−6353.
(18) Perez-Paya, E.; Houghten, R. A.; Blondelle, S. E. *J. Biol. Chem.* **1996**, *271*, 4120−4126.
(19) Aggeli, A.; Bell, M.; Boden, N.; Keen, J. N.; Knowles, P. F.; McLeish, T. C. B.; Pitkeathly, M.; Radford, S. E. *Nature* **1997**, *386*, 259−262.
(20) Clark, T.D.; Buriak, J. M.; Kobayashi, K.; Isler, M. P.; McRee, D. E.; Ghadiri, M. R. *J. Am. Chem. Soc.* **1998**, *120*, 8949−8962.
(21) Fujita, K.; Kimura, S.; Imanishi, Y. *Langmuir* **1999**, *15*, 4377−4379.
(22) Maget-Dana, R.; Lelievre, D.; Brack, A. *Biopolymers* **1999**, *49*, 415−423.
(23) Powers, E. T.; Kelly, J. W. *J Am. Chem. Soc.* **2001**, *123*, 775−776.
(24) Wattenbarger, M.R.; Chan, H. S.; Evans, D. F.; Bloomfield, V. A.; Dill, K. A. *J. Chem. Phys* **1990**, *93*, 8343−8351.
(25) Chan, H. S.; Wattenbarger, M. R.; Evans, D. F.; Bloomfield, V. A.; Dill, K. A. *J Chem. Phys.* **1991**, *94*, 8542−8557.
(26) Tsuchiya, K.; Takahashi, A.; Takeda, N.; Asakawa, N.; Kuroki, S.; Ando, I.; Shoji, A.; Ozaki, T. *J. Mol. Struct.* **1995**, *350*, 233−240.
(27) Gregory, D. M.; Mitchell, D. J.; Stringer, J. A.; Kiihne, S.; Shiels, J. C.; Callahan, J.; Mehta, M. A.; Drobny, G. P. *Chem. Phys. Lett.* **1995**, *246*, 654−663.
(28) Mehta, M. A.; Gregory, D. M.; Kiihne, S.; Mitchell, D. J.; Hatcher, M. E.; Shiels, J. C.; Drobny, G. P. *Solid State Nucl. Magn. Reson.* **1996**, *7*, 211−228.
(29) Gregory, D. M.; Mehta, M. A.; Shiels, J. C.; Drobny, G. P. *J. Chem. Phys.* **1997**, *107*, 28−42.
(30) Bower, P. V.; Oyler, N.; Mehta, M. A.; Long, J. R.; Stayton, P. S.; Drobny, G. P. *J. Am. Chem. Soc.* **1999**, *121*, 8373−8375.

a 2-ms mixing time. Applying a DRAWS pulse sequence for 3−6 ms, using a ^{13}C field of 34.0 kHz, generates dipolar-correlated spin coherence ($I_xS_z \pm S_xI_z$). Applying a 90° pulse then generates double-quantum coherence. In the double-quantum buildup experiment, this coherence is immediately transferred back to antiphase magnetization by a second 90° pulse and then to observable magnetization by reapplying the DRAWS mixing sequence for the same amount of time. The buildup of double-quantum coherence was then monitored as a function of the DRAWS mixing time to determine dipolar couplings. Proton decoupling of >110 kHz was applied throughout the DRAWS, evolution, and acquisition periods. The samples were spun at 4000 ± 5 Hz to match with the 250-μs DRAWS cycle time. Each double-quantum buildup experiment was run at least 5 times, and each time point was signal-averaged for either 128 (neat peptide) or 1024 (peptide on polystyrene) scans per spectrum using a repetition time of 4 s.

In the two-dimensional DQDRAWS experiment, the DRAWS pulse sequence is again applied for 4−6 ms, depending on the distance between the isotopically labeled carbonyl carbons, to generate the antiphase state. After the magnetization is transferred to the double-quantum state by a 90° pulse, it is allowed to evolve under the chemical shift and dipolar interactions for 0−3 ms, corresponding to 120 t_1 time points with a dwell time of 25 μs. The magnetization is then transferred back to an observable state by a second 90° pulse and reapplying the DRAWS mixing sequence for the same amount of time. Proton decoupling of >110 kHz was applied throughout the DRAWS, evolution, and acquisition periods. The samples were spun at 4000 ± 5 Hz to match with the 250-μs DRAWS cycle time. Each time point was signal-averaged for either 128 (neat peptide) or 512 (peptide on polystyrene) scans per spectrum using a repetition time of 4 s. The DQDRAWS were simulated as a function of t_1 evolution using code previously described operating in a Matlab environment. Torsion angle values were obtained from a least-squares minimization of the evolution in the t_1 dimension. Simulations incorporated the observed chemical shift anisotropies, experimental parameters, and principal axes of the CSAs relative to the amide bonds (molecular frame) as previously described.

Results

Peptide Adsorption to Polystyrene and Chemical Shift Analysis. Qualitative information about peptide secondary structure may be determined by measuring isotropic chemical shifts and the chemical shift anisotropy (CSA) tensor.[31−36] A chemical shift analysis of peptide structure, both lyopholized and on the polystyrene surface, was initially performed as a function of peptide concentration in solution. It was observed that relatively high concentrations of peptide in solution were necessary to drive appreciable adsorption onto the high-surface-area polystyrene. At all concentrations, the peptides remained in solution, indicating any aggregates forming were limited in size. This behavior was previously seen in solutions of similar peptides.[16] Figure 1 shows the ^{13}C chemical shift spectra of the $LK3_{10}7$ peptide when it was lyophilized from dilute solution, lyophilized from concentrated solution, and adsorbed on polystyrene from a concentrated solution. A double-quantum-filtered spectrum of the peptide adsorbed on polystyrene is also shown for comparison. Although only 30% of the signal from the isotope- enriched carbonyl carbons is recovered in the double-quantum experiment, sufficient signal is obtained and the interpretation of the spectrum is greatly simplified because all contributions from natural-abundance carbon in the peptide and polystyrene are removed.

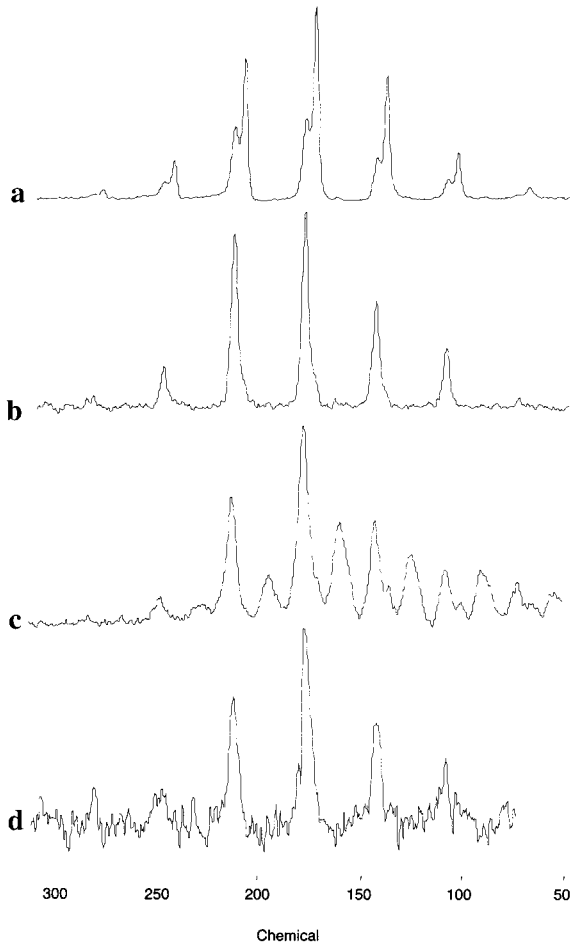

Figure 1. CPMAS and DQ filtered spectra of the carbonyl region in Ac-LLKLLKL-NH_2 after different sample preparations: (a) CPMAS of peptide lyophilized from a dilute (<100 uM) solution, (b) CPMAS of peptide lyophilized from a concentrated (>1 mM) solution, (c) CPMAS of peptide adsorbed on polystyrene, and (d) DQ filtered spectrum of peptide adsorbed on polystyrene.

In both the spectra of the peptide on polystyrene and the peptide lyophilized from a concentrated solution, the isotope-enriched carbonyl carbons have a chemical shift of 177 ppm and a chemical shift anisotropy of 0.6. Previously it was shown that these values correlate to helical structure in peptides.[34] In contrast, the spectrum of the peptide lyophilized from a dilute solution shows two distinct resonances—a sharp peak at 177 ppm ($\eta = 0.6$) and a broader peak at 172 ppm ($\eta = 0.9$). These correspond to helical and random coil conformations, respectively.

These results indicate that aggregation and formation of secondary structure in solution precedes adsorption onto the polystyrene surface. Given the relatively small sizes of the peptides, this concentration dependence is not unexpected. Similarly, the other three peptides were found to have little secondary structure or affinity for polystyrene at low concentrations (<1 mM). At higher concentrations (> 1 mM), the peptides aggregated with well-defined secondary structures and subse-

(31) Asakawa, N.; Kurosu, H.; Ando, I.; Shoji, A.; Ozaki, T. *J. Mol. Struct.* **1994**, *317*, 119−129.
(32) Tsuchiya, K.; Takahashi, A.; Takeda, N.; Asakawa, N.; Kuroki, S.; Ando, I.; Shoji, A.; Ozaki, *T. J. Mol. Struct.* **1995**, *350*, 233−240.
(33) Kameda, T.; Takeda, N.; Kuorki, S.; Kurosu, H.; Ando, S.; Ando, I.; Shoji, A.; Ozaki, T. *J. Mol. Struct.* **1996**, *384*, 17−23.
(34) Ando, I.; Kuroki, S. *The Encyclopedia of NMR.*; John Wiley: New York, 1996; pp 4458−4463.
(35) Kameda, T.; Ando, I. *J. Mol. Struct.* **1997**, *412*, 197−203.
(36) Ando, I.; Kameda, T.; Asakawa, N.; Kuroki, S.; Kurosu, H. *J. Mol. Struct.* **1998**, *441*, 213−230.

Table 1. Isotropic Chemical Shifts of Labeled Carbonyl Carbons, Carbonyl Carbon Chemical Shift Anisotropies (δ, η), Distance Measurements between Carbonyl Carbon Labels, and Torsion Angles (φ, ψ) Measured via Relative Orientations of the Carbonyl Carbon CSA Tensors

	periodicity	CS (ppm)	CSA (δ, η)	distance (Å)	(φ, ψ) (deg)
		Peptide Lyophilized from > 1 mM Solution			
Ac-LLKK**LL**KL-NH_2	α-helix	176[a]	150,[a] 0.6[a]	3.06 ± 0.1[b]	(-72 ± -3,[c] -29 ± -1[d])
Ac-LKKLLK**LL**KKLLKL-NH_2	α-helix	177	150, 0.6	3.01	(-63 ± 1, -39 ± 1)
Ac-LLK**LL**KL-NH_2	3_{10}-helix	176	151, 0.6	3.10 ± 0.15	(-78 ± 2, -21 ± 1)
Ac-LLK**LL**KLLKLLKL-NH_2	3_{10}-helix	177	149, 0.6	3.02	(-65 ± 1, -36 ± 1)
		Peptide on Polystyrene			
Ac-LLKK**LL**KL-NH_2	α-helix	177	145, 0.6	3.02	(-64 ± 11, - - -)
Ac-LKKLLK**LL**KKLLKL-NH_2	α-helix	177	145, 0.6	3.00	(-62 ± 6, -34 ± 2)
Ac-LLK**LL**KL-NH_2	3_{10}-helix	177	145, 0.6	3.07	(-70 ± 11, - - -)
Ac-LLK**LL**KLLKLLKL-NH_2	3_{10}-helix	177	145, 0.6	3.05	(-67 ± 7, -33 ± 2)
		Peptide Lyophilized from <100 μM Solution			
Ac-LLKK**LL**KL-NH_2	α-helix	173	150, 0.9		
Ac-LKKLLK**LL**KKLLKL-NH_2	α-helix	173	150, 0.9		
Ac-LLK**LL**KL-NH_2	3_{10}-helix	173	149, 0.9		
Ac-LLK**LL**KLLKLLKL-NH_2	3_{10}-helix	173	150, 0.9		

[a] All results are reported to the last significant digit. [b] Average and dispersion of distances observed for the sample, as described in ref 44. [c] Errors in φ correspond to $\sigma = 1$ in the χ^2 analysis of the dipolar recoupling data with simulations. The error in each data point corresponded to the rms noise in the experimental spectrum. [d] Errors in ψ correspond to $\sigma = 1$ in the χ^2 analysis of the 2D DQDRAWS data with simulations. The error in each data point corresponded to the rms noise in the experimental spectrum. The torsion angle φ was held to the value determined from the dipolar recoupling data.

quently adsorbed to polystyrene at a much higher level. This behavior is reminiscent of other amphipathic molecules such as lipids, where surface adsorption from micelles has been extensively studied. However, the formation of hydrogen-bonding networks in these peptide aggregates yields an added degree of control/complexity in the self-assembly characteristics.[17−21] It should be noted that at even higher concentrations (10 mM) the helical peptides remain soluble, suggesting the formation of helical bundles with a limited size distribution. Similar systems making use of β-sheet-type structures have exhibited aggregation out of solution.[16−17,19] This may hinder their adsorption in systems making use of porous, high-surface-area polymers.

Peptide Dynamics on Polystyrene. The CSA values can also provide information about the presence of dynamics. As mobility increases, the anisotropy will become increasingly averaged until it approaches the liquid-state spectrum, the completely averaged or isotropic state. As is evident in Figure 1 and Table 1, the CSAs indicate that there is little or no peptide motion on the time scale (<kHz) of the NMR experiments even for the shorter peptides. Measurement of the ^{13}C $T_{1\rho}$ relaxation constants[37] (data not shown) and the buildup of double-quantum efficiency in the DQDRAWS experiment also indicate there is no detectable motion of the adsorbed peptides on the time scales of the experiments. To determine whether this was true for the entire lengths of the peptides, a second LKα8 peptide was synthesized with the carbonyl carbon labels placed at the N-terminus. CPMAS spectra of this peptide adsorbed on polystyrene were indistinguishable from those of the LKα8 peptide isotopically enriched in the middle of the sequence. Taken together, these findings demonstrate that the peptides are tightly bound to the surface along their sequence. This is in contrast to what we have observed previously for peptides adsorbed on ionic surfaces.[38]

Dipolar Recoupling Analysis of Peptide Structure. Higher resolution determination of the secondary structure of these peptides was accomplished by using the DRAWS SSNMR experiment to measure φ and DQDRAWS SSNMR experiment for simultaneous measurement of (φ, ψ). Figure 2 shows the DRAWS results for the peptides lyophilized from concentrated solutions. The projections along the double-quantum axis for the 2D DQDRAWS experiments on the LKα14 and $LK3_{10}7$ lyophilized aggregates are shown in Figure 3. The secondary structure characteristics of all the peptides are summarized in Table 1. While all the peptides were observed to have similar

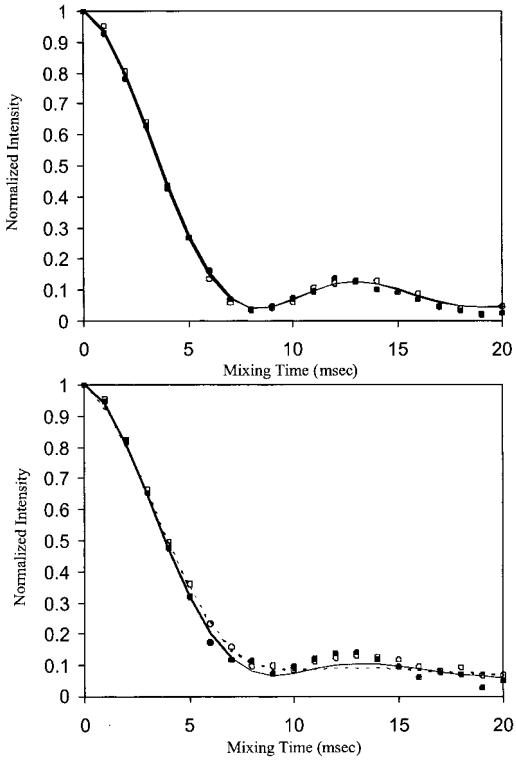

Figure 2. DRAWS dephasing curves for peptides lyophilized from concentrated solutions: (a) Longer helices Ac-LKKLLKLLKKLLKL-NH_2 (●) and Ac-LLKLLKLLKLLKL-NH_2 (○) and simulations for ϕ torsion angles of −63° and −65°. (b) Shorter helices Ac-LLKKLLKL-NH_2 (●) and Ac-LLKLLKL-NH_2 (○) and simulations for ϕ torsion angles of −72° with a SD of 20° and −78° with a SD of 30°.

(37) Schaefer, J.; Stejskal, E. O.; Buchdahl, R. *Macromolecules* **1977**, *10*, 384−405.
(38) Shaw, W. J.; Long, J. R.; Campbell, A. A.; Stayton, P. S.; Drobny, G. P. *J. Am. Chem. Soc.* **2000**, *122*, 7118−7119.

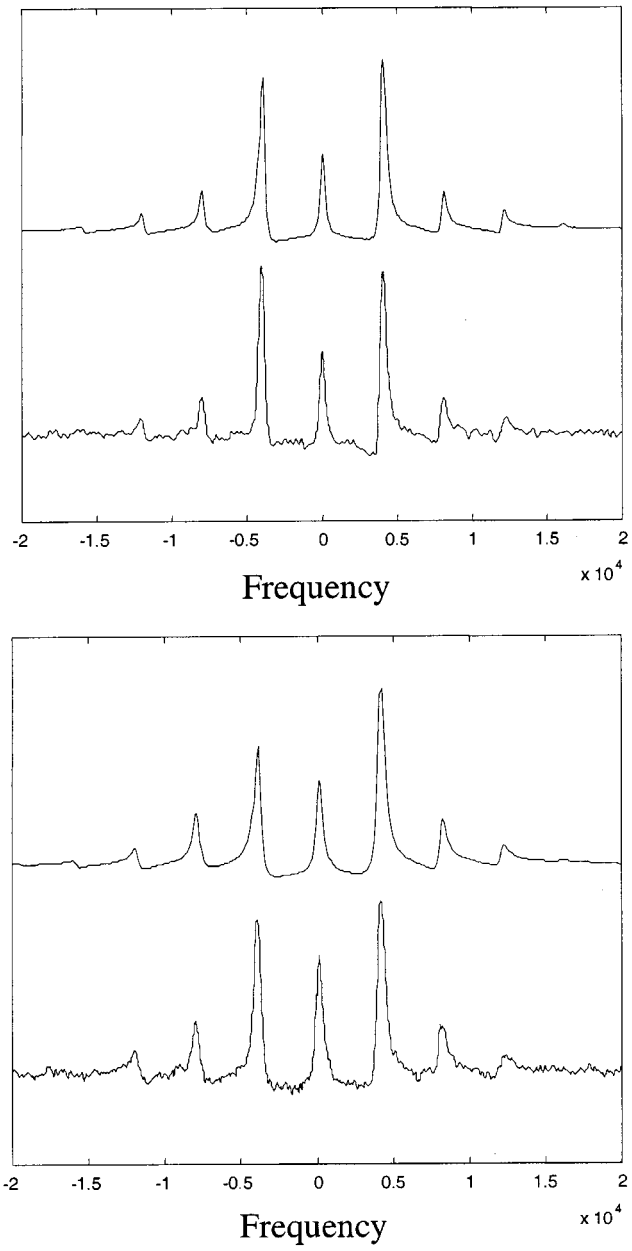

Figure 3. Projections of 2D DQDRAWS spectra onto the double-quantum axis for peptides lyophilized from concentrated solutions: (a) Ac-LKKLLKLLKKLLKL-NH_2 and (b) Ac-LLKLLKL-NH_2 along with simulations for (−63°, −39°) and (−78°, −21°), respectively.

chemical shifts and anisotropies, clear distinctions begin to emerge from the higher resolution data. Notably, helix length, rather than hydrophobic periodicity, determines whether the helices are more or less α-helical in character. The only peptide with torsion angle ψ approaching that expected for a 3_{10}-helix is the seven-amino acid peptide with the corresponding hydrophobic repeat, $LK3_{10}7$ (−78 ± 2°, −21 ± 1°). The shorter α-helical repeat peptide LKα8 (−72 ± 3°, −29 ± 1°) also shows some tendency toward torsion angles intermediate between a typical α-helix (−62°, −41°) and 3_{10}-helix (−71°, −18°).[39] Both the shorter peptides displayed some heterogeneity in their structures. Analyses of the DRAWS data indicate Gaussian distributions of φ torsion angles characterized by standard deviations from the average φ torsion angles on the order of 12° and 17° for LKα8 and $LK3_{10}7$, respectively. However, both the longer helical peptides, LKαl4 (−63 ± 1°,−39 ± 1°) and $LK3_{10}13$ (−65 ± 1°, −36 ± 1°), have torsion angles similar to those expected for α-helices with little or no structural heterogeneity. This is in good agreement with previous observations of helical propensities.[40,41] However, it should be noted these peptides are forming aggregates in solution.

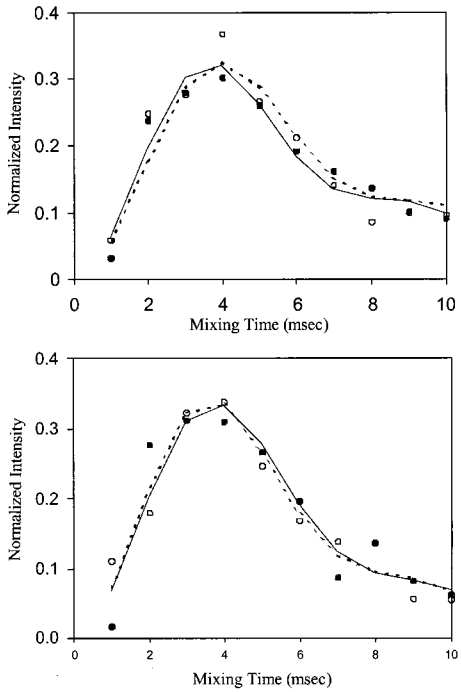

Figure 4. DQDRAWS buildup curves for hydrated, surface-adsorbed peptides on polystyrene: (a) Longer helices Ac-LKKLLKLLKKLLKL-NH_2 (●) and Ac-LLKLLKLLKLLKL-NH_2 (○) and simulations for ϕ torsion angles of −62° and −67°. (b) Shorter helices Ac-LLKKLLKL-NH_2 (●) and Ac-LLKLLKL-NH_2 (○) and simulations for ϕ torsion angles of −64° and −70°.

When the peptides are adsorbed on polystyrene, a significant natural-abundance contribution from the aromatic groups in polystyrene complicates any quantitative analysis of single-quantum spectra. Thus, the double-quantum buildup experiment was used to measure the distances between adjacent carbonyl carbons in the peptides backbones. Figure 4 displays the buildup of double-quantum coherence for the four peptides adsorbed on polystyrene. Two-dimensional DQDRAWS spectra were also obtained for the longer peptides, and the results for these peptides, LKαl4 and $LK3_{10}13$, are shown in Figure 5. The S/N ratios for the shorter peptides were significantly poorer, due to less adsorption to the surface. Consequently, only the DQ buildup was monitored.

The results obtained for the four peptides adsorbed to polystyrene are fairly similar to those for the peptide aggregates and demonstrate that all the peptides are helical when adsorbed to the surface. However, the torsion angles measured in the peptides adsorbed on polystyrene differ slightly from those measured for the aggregates. For the $LK3_{10}13$ peptide, φ increased from −65 ± 1° to −67 ± 7° and ψ decreased from −36 ± 1° to −33 ± 2°. For the LKα14 peptide, φ decreased from −63 ± 1° to −62 ± 6° and ψ decreased from −39 ± 1°

(39) Barlow, D. J.; Thornton, J. M. *J. Mol. Biol.* **1988**, *201*, 601−619.
(40) Karle, I. L.; Flippen-Anderson, J. L.; Gurunath, R.; Blaram, P. *Protein Sci.* **1994**, *3*, 1547−1555.
(41) Millhauser, G. L. *Biochemistry* **1995**, *34*, 3873−3877.

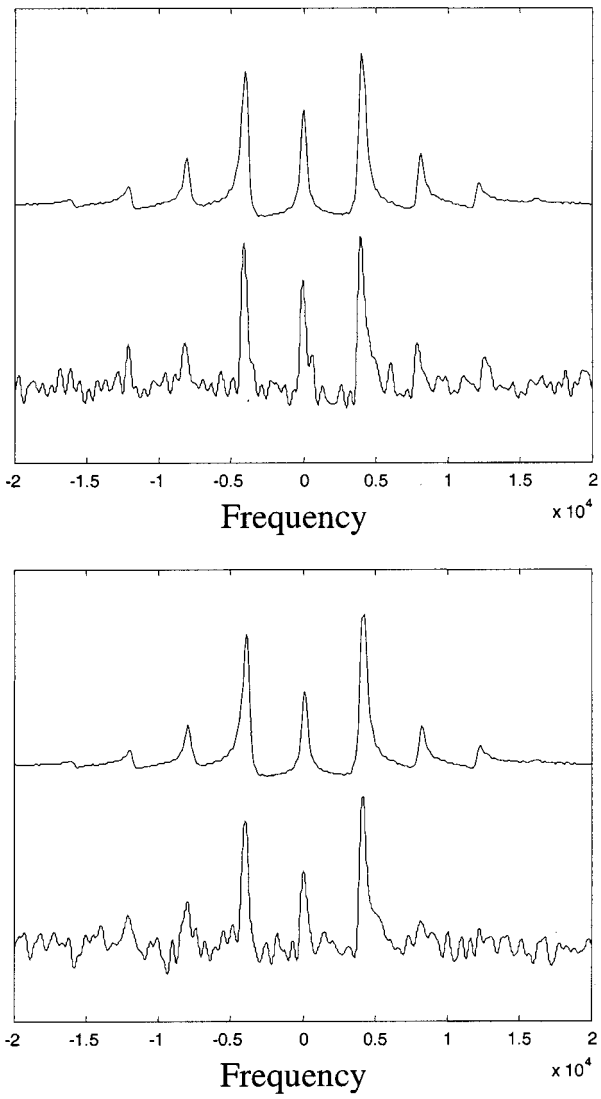

Figure 5. Projections of 2D DQDRAWS spectra onto the double-quantum axis for hydrated peptides adsorbed on polystyrene: (a) Ac-LKKLLKLLKKLLKL-NH_2 and (b) Ac-LLKLLKLLKLLKL-NH_2 along with simulations for (−62°, −34°) and (−67°, −33°), respectively.

to $-34 \pm 2°$. For the shorter peptides, φ decreased in both cases—from $-72 \pm 3°$ to $-64 \pm 11°$ for LKα8 and from $-78 \pm 2°$ to $-70 \pm 11°$ for $LK3_{10}7$. These changes indicate adsorption on polystyrene may induce more helical structure in the shorter peptides and that slight changes in torsion angles are needed for the longer peptides to adsorb on the polystyrene surface.

Discussion

Our long-term goal is to design well-structured and oriented peptide or protein surface coatings on biomaterial, tissue engineering, and device surfaces (e.g., diagnostic, chip, microfluidic channels). Being able to control their structure and orientation on the surface will enhance their ability to display signal sequences that interact with target cell receptors, to display larger proteins on chip surfaces, and to open avenues for templating off specific side-chain residues that have defined periodicity. One particularly important application is in the surface modification of three-dimensional, porous scaffolds for tissue engineering.[42,43] Immobilization chemistry is difficult in these complex structures, but peptides that bind tightly in ordered and oriented fashion from solution may allow better penetration and coverage.

Here we have utilized periodic peptide sequences first designed and shown to form helical structures at the air/water interface by DeGrado and co-workers. This suggested that they may also fold into defined helices on hydrophobic surfaces such as polystyrene, although the mechanistic assembly process could be very different. A key component of the approach described in this paper is the verification of structure on the relevant biomaterial surfaces using solid-state NMR. Vibrational and optical spectroscopies have provided important structural information, primarily with regard to secondary structure content and protein unfolding on surfaces. However, such methods can only detect averaged secondary structures, and they provide little dynamic information. Many vibrational and optical spectroscopies are also limited by their inability to probe rough or porous structures.

Solid-state NMR can provide high-resolution structural and dynamic information about peptides on hydrated surfaces. DRAWS is well suited to measuring distances between adjacent backbone carbonyl carbons in peptides and proteins. Based on these distance measurements, the torsion angle φ may be determined at several positions in a peptide in a model-independent fashion. Additionally, DRAWS can also measure conformational heterogeneity since the dipolar recoupling efficiency is independent of any correlation between chemical shift and peptide secondary structure.[28,44] This allows the determination of the distribution of peptide conformers in a given sample.

DQDRAWS is a pulse experiment that utilizes DRAWS recoupling to generate double-quantum coherence between two homonuclear spins. Monitoring the generation of the double-quantum coherence as a function of DRAWS mixing time allows determination of the distance between the two spins. Although this technique has lower sensitivity than the single-quantum DRAWS experiment, it has the added benefit of filtering out any contributions from the natural-abundance background. This provides significant advantage in highly heterogeneous systems where the molecules of interest comprise a small fraction of the entire sample. Once a double-quantum coherence is generated, it can then evolve under the influence of the dipolar coupling between these spins and the tensor sum of their respective CSAs before being converted back to a single-quantum state for observation. Since carbonyl carbons in peptides possess highly anisotropic CSAs, they are particularly sensitive to this technique. The relative orientations of the carbonyl carbon CSAs to the peptide amide bonds is well understood, and thus, the torsion angles (φ, ψ) can be extracted by simulating the DQ spectrum. Determining (φ, ψ) with this level of accuracy not only yields secondary structure but also gives some indication of helical pitch or twist and long-range order.

The combination of CPMAS, CSA, DRAWS, and DQDRAWS techniques elucidated the molecular structure and dynamics of

(42) Brauker, J. H.; Carr-Brendel, V. E.; Martinson, L. A.; Crudele, J.; Johnston, W. D.; Johnson, R. C. *J Biomed. Mater. Res.* **1995**, *29*, 1517−1524.
(43) Sieminski, A. L.; Gooch, K. J. *Biomaterials* **2000**, *21*, 2233−2241.
(44) Shaw, W. J.; Long, J. R.; Dindot, J. L.; Campbell, A. A.; Stayton, P. S.; Drobny, G. P. *J Am. Chem. Soc.* **2000**, *122*, 1709−1716.

the LK peptides in solution and on the polystyrene surface. This work emphasizes the complexity of the interaction between peptides and hydrophobic surfaces. An equilibrium exists between unfolded peptides and folded peptide assemblies in solution, as well as between the soluble peptide assemblies and adsorbed peptides. Once the peptides adsorb irreversibly on the surface from aqueous solution, they are immobile on the NMR time scale along the entire length of the peptide. For the longer peptides, structural measurements indicate adsorption is accompanied by a slight change in the backbone torsion angles. This may be a consequence of the peptides adsorbing on an immobile, two-dimensional surface rather than interacting with other flexible peptides to reach an energy minimum. The change in torsion angles from (−63°, −39°) and (−65°, −36°) to (−62°, −34°) and (−67°, −33°) in the Lkα14 and $LK3_{10}13$ peptides, respectively, indicates conformational changes leading to the leucines being more aligned along one side of the peptides. This adjustment likely maximizes interactions with the hydrophobic surface.

Because these peptides bind tightly to hydrophobic surfaces with defined structure and little dynamics, they may serve as useful adaptors for materials coatings. By forming specific secondary structures on hydrophobic surfaces using the hydrophobic effect, the solvent-exposed helical face can also be utilized for orthogonal chemistry (indeed, the lysine residues themselves provide primary amines for chemical linkages), to control electrostatic properties, spacing of pendant molecules, etc. Modifying the choice of hydrophobic side chains may also optimize the strength of the interaction between the peptides and the surface. We are currently investigating the use of these adaptors as a route for immobilizing fusion sequences and as templates for subsequent derivitization.

Acknowledgment. We gratefully acknowledge the support provided by the National Science Foundation (Grants EEC-9529161 and DMR-9616212) and by the National Dental Institute (Grant DE 12554).

JA011624N